ADVANCED PROCESS MODELING AND SIMULATION OF MULTI-MATERIAL DIRECTED ENERGY DEPOSITION

E. OSMANOGLU*, C. CANAZ**, N. HEMPEL***, P. MAYR****

**Technical University of Munich, Chair of Materials Engineering of Additive Manufacturing, 85748, Garching, Germany, 0000-0003-3868-5407, emre.osmanoglu@tum.de*
*** Technical University of Munich, Chair of Materials Engineering of Additive Manufacturing, 85748, Garching, Germany, 0009-0001-7704-674X*
****Technical University of Munich, Chair of Materials Engineering of Additive Manufacturing, 85748, Garching, Germany, 0000-0001-7316-1065*
*****Technical University of Munich, Chair of Materials Engineering of Additive Manufacturing, 85748, Garching, Germany, 0000-0003-2530-4644*

DOI 10.3217/978-3-99161-089-2-012,

ABSTRACT

As technology advances, materials face increasing demands, especially in the aerospace industry. Metal additive manufacturing (AM), specifically directed energy deposition (DED), addresses these needs by enabling multi-material deposition and in-situ alloying, producing functionally graded materials (FGMs) with tailored properties by combining different materials. Numerical simulations can be used to predict temperature fields and distortions in the DED process, reducing costly trial runs. However, incorporating FGMs in such thermomechanical simulations of DED process requires development of new process models and creation of material models for specific alloy combinations. Using Simufact Welding and extending the capabilities of the software, a DED process is modelled, and material compositions are assigned to layers to construct FGMs virtually in this work. Initial process simulations of CuCrZr-IN718 FGM deposition on a CuCrZr substrate demonstrate successful modelling of the process. These models correlate well with experimental results, predicting temperature fields and distortions effectively. Future work includes further validation and scaling simulations for industrial applications.

Keywords: Directed energy deposition, functionally graded materials, process simulation, multi material additive manufacturing

INTRODUCTION

In aerospace applications, parts have to perform under extreme conditions. A way to address these challenges is to build multi-material structures that are made of functionally graded materials (FGM) [1-3]. Various additive manufacturing (AM) methods are used to build FGM structures such as laser directed energy deposition [4-6] and wire arc additive manufacturing [7-8]. In this work, the FGM will be built by combining CuCrZr with IN718, using plasma directed energy deposition or 3D plasma metal deposition (3DPMD).

While there is previous work on multi material metal AM, process digitalization is a relatively underdeveloped area. The goal of process simulation in DED of metals is to predict the temperature field distribution of the printed structure, to calculate the residual stress and resulting distortions as accurately as possible. The simulations also demonstrate the connection between the process parameters, used materials and resulting temperature and stress fields [9-10]. By calibrating the heat source model and the simulation process parameters, it is aimed to provide a representative model that can be used to minimize resulting stress and distortions on the printed body without the costly and time-consuming experimental procedures.

Finite element method (FEM) is a widely used approach for simulating thermomechanical behavior of parts built via DED. It enables the prediction of fields that determine the part's performance, such as temperature distribution, residual stress, and geometric deformation [9-10]. Many finite element (FE) models representing a DED process include the key properties:

- Moving heat source models, such as Goldak or cylindrical types
- Element activation/deactivation technique to model layer-by-layer material deposition
- Adaptive meshing around heat affected zone (HAZ)
- Path-based simulation to mimic heat source movement
- Thermo-mechanical coupling for stress-strain analysis

These well-established numerical methods allow detailed analysis of the DED process. In recent developments, these models are often augmented with machine learning-based surrogate models to improve computational efficiency and gain new insights [11].

In this work, the established simulation methods will be extended to incorporate multi-material deposition process, which is used to manufacture FGMs. For this purpose, new material models will be generated by combining the existing material models using rule of mixtures.

PROCESS DIGITALIZATION

To simulate large-scale additive manufacturing builds, Ref. [9] created a thermomechanically coupled FE model, concentrating on electron beam deposition of Ti–6Al–4V. To demonstrate the progressive layer-wise addition of material, their model used also a sequential element activation technique and included an elastoplastic material formulation. In this technique, elements representing the deposited material are initially removed, then reintroduced layer by layer in an inactive state. They are activated with their true material properties as the moving energy source approaches. To overcome the computing difficulties of simulating more than 100 layers, authors developed an adaptive meshing approach that greatly reduced the total degrees of freedom by coarsening the mesh in previously deposited regions while maintaining fine resolution close to the melt pool. A moving volumetric heat source was used to simulate the thermal input, and the temperature distribution, residual stress, and deformation during the printing process were calculated. With prediction errors of less than 29%, validation against experimental distortion measurements were promising. This work offers a computationally effective method for simulating industrial-scale builds, marking a significant leap in the numerical simulation of metal additive manufacturing. Since then, it has been used as a basis for the advancement of adaptive meshing algorithms and element activation techniques in both commercial and research DED simulation systems.

Ref. [12] studied how to simplify the modelling of transient heat source motion in thermomechanical finite element simulations for DED. They used Simufact Welding 2021.1 to model laser DED of an 80-layer stainless steel turbine blade. They suggested the Advanced Thermal Cycle (ATC) method, which groups several thermal increments to simulate the heat input over greater regions. Their results showed that the predicted thermal fields and geometric distortions aligned well with experimental results even when significant simplifications were applied (e.g., 10 to 100 increments grouped together). Grouping 10 increments reduced computation time by up to 90% while keeping the predicted geometry accurate. The study showed that ATC is an effective method for making DED simulations faster, while still maintaining good model quality for industrial use.

As of lately, functionally graded materials (FGMs) have also become a big focus in DED processes. Rather than relying on a single material with uniform properties, the ability to vary the composition and microstructure throughout a printed part has shown great promise in high-performance demanding areas like aerospace. Ref. [13] worked on thermomechanical modelling of two FGM cases manufactured via laser DED with direct deposition of Copper on SS304L, and a functionally graded material (FGM) structure transitioning from SS316L to IN718 to Copper on an SS304L substrate. During the process, temperature data from the substrate was gathered to calibrate and validate the 3D thermomechanical model. Then the resulting distortions and stresses were analysed. Numerical and experimental temperature histories aligned well, with the accuracy increasing as the layers progress. The developed model can predict stress in single material DED parts accurately and help choose better designs and materials.

In this work, the 3DPMD process will be digitalized using Simufact Welding software. In the digitalization process, substrate, clamping solution, and heat source will be transferred to the digital environment and the simulated process will be run according to the process parameters coming from the experiments.

The digitalization that is proposed in this work follows calibration, validation, and simulation steps. In the calibration step, the heat source will be calibrated according to experiment. In the validation step, a new validation experiment is conducted to assess the accuracy of the digital model and determine if the model is overfitted to a specific case. Finally, multi material deposition of a structure made of Cu-Ni FGM by the 3DPMD process is simulated. It will be demonstrated that the proposed method of process digitalization yields accurate time-temperature history with an error less than 10% and generates a model that is not overfitted to a specific case but can be used for different deposition conditions using same equipment.

EXPERIMENTAL SETUP

The 3DPMD process is conducted using a torch attached to a six-axis industrial robot. The substrates are clamped to the base of the industrial robot. Two different powder feedstocks can be simultaneously supplied to the plasma torch to achieve in-situ alloying.

In the experiments argon is used for plasma gas, shielding gas and transportation gas. The powders of CuCrZr and IN718 have the particle sizes 90% 45-100 µm and 45-106 µm, respectively. The chemical compositions of the powders are given in Table 1.

Table 1 Chemical compositions of the powders in weight percentages

Element	Ni	Cu	Cr	Zr	Fe	Si	Ti	Nb	Mo
IN718	53.2	0.01	18.99	-	17.73	0.21	1.01	5.02	3.13
CuCrZr	-	Bal.	0.77	0.09	0.01	0.01	-	-	-

The substrate plate is heated up to 350 °C using a heating plate. It is then transferred to the robot based and clamped for the deposition process. The welding is started when the plate cools down to 300 °C, which corresponds to interlayer temperature. During the process, this interlayer temperature of 300 °C is controlled using a pyrometer. The pyrometer was calibrated by measuring the surface temperature of the substrate with a thermocouple. In addition to the pyrometer, the temperature of the substrate was recorded with thermocouples. The location and the orientation of the thermocouples at the multi-material experiment are presented in Fig. 1. In the calibration and validation experiments, thermocouples are attached to substrate from bottom. Holes with a depth of 5 mm drilled on the substrate to locate the thermocouples to the surface as close as possible. The location of the thermocouples for the calibration and validation experiments are presented in Fig. 2 and Fig. 3, respectively.

Fig. 1 Multi material DED deposition of IN718 on a CuCrZr substrate with thermocouples for temperature measurement. Bright point on the top left surface of the deposition is the laser of pyrometer.

The process parameters used for deposition of CuCrZr and IN718 is presented in Table 2. For the transition layers, CuCrZr and IN718 mixed in equal proportions by weight. The deposition is further explained at the corresponding experiment.

Table 2 Process parameters for the deposition of CuCrZr and IN718

Process Parameter	Details
Welding speed	2 mm/s
Line energy for CuCrZr	2.75 – 2.60 kJ/mm
Line energy for transition zone	2.45 kJ/mm
Line energy for IN718	2.20 kJ/mm
Powder supply rate	24.3 g/min
Layer height	2.5 mm
Standoff distance	10 mm
Plasma gas flow rate	1.5 L/min
Shielding gas flow rate	15 L/min
Preheating temperature	300 °C
Dwell time between layers	300 – 60 s

In the simulations, material models from the materials library of the Simufact Welding are used for CuCrZr and IN718. The material model for the gradient is obtained by mixing the two materials according to the rule of mixtures, which will be discussed in the corresponding chapter.

SIMULATION MODEL CALIBRATION

In the process calibration step, the digital model of the 3DPMD process is created in Simufact Welding. The main aspect of this step is the calibration of the heat source. The process parameters and the geometries of substrate and deposition are known inputs for the simulation, but the heat source is an unknown. While the dimensions of the heat source dictate the deposition geometry, the efficiency of the heat source scales the heat source power, which affects the time-temperature history.

The first step of the process digitalization is the generation of geometries in the simulation software. In the calibration simulation, only substrate and deposited wall is modelled because the clamping was minimal in the experiments. The simulation model is presented in Fig. 2. This model contains deposition wall, substrate, heat source model, and clamping models.

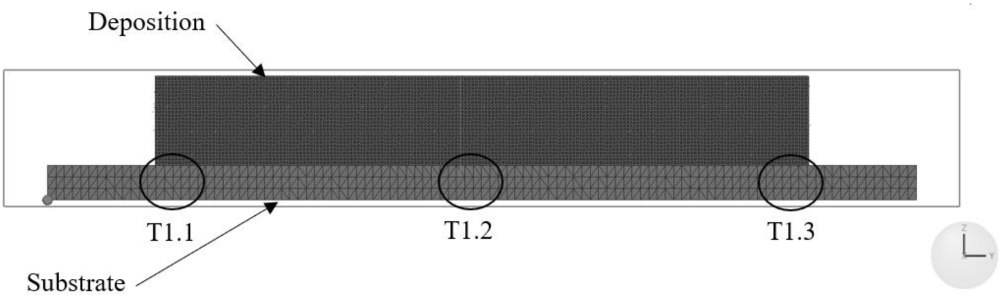

Fig. 2 Simulation model for the calibration runs. Thermocouples T1.1-3 are attached from the bottom of the substrate, 5 mm deep along the center line of the deposition.

During the experiment, layer dimensions depend on the standoff distance between the torch and the substrate surface. This distance is kept constant at 10 mm but due to the different powder capture efficiencies during the deposition of consecutive layers, the layer height changes ±0.5 mm during the process. For the simulations, a uniform layer height is assumed by dividing the height of the deposited wall to the number of layers, which is 2.5 mm.

In the calibration simulations, heat source size is determined according to the width and the height of the deposited layers. A disk type heat source is generated to encompass the deposition track. The height and radius of the disk are increased by 10% to ensure that the disk can cover the deposition tracks completely and achieve some penetration between the consecutive layers.

For the calibration of the simulation multiple simulation runs were conducted. The goal of the calibration is to match the time-temperature history from the simulations with the measurements from the experiments. In the time-temperature history, peaks correspond to the instances at which the torch is in-line with the thermocouple. Therefore, one must adjust the heat source efficiency to match the peaks. The second aspect of time-temperature history is the cooling behaviour. As the heat source moves away from the thermocouple, the temperature reading starts to drop. This is due to the heat dissipation within the part and heat loss to the environment. Hence, to have an accurate simulation, these factors must be modelled accurately.

First a mesh sensitivity analysis is conducted to eliminate uncertainty associated with mesh size. Then, the efficiency of the heat source is adjusted so that the peaks of the simulated time-temperature history match the measured values. While calibrating the heat source efficiency, the melt pool temperature was also checked to ensure that the temperature surpassed the melting point of the CuCrZr.

The cooling of the deposition did not require an extensive calibration like the heat source as the clamps are omitted in the simulation model. The convection coefficient between the deposition and the environment is calculated to be 19.9 W/m^{2}K based on the temperature drop rate. The recommended value in the literature for the convection coefficient is 20 W/m^{2}K [14], which is also the built-in value in the simulation software. Hence, the software recommendation was used in the simulations.

The comparison of the time-temperature measurement with the simulated values for the first layer of the deposition is presented in Fig. 3. The simulated values do not perfectly fit with measured values because of the dimensional inaccuracy. In the experiments, thermocouples were attached to the substrate from the holes drilled to the bottom of the plate. During the deposition process, the orientation of the substrate was not as accurate as the simulations due to the minimal clamping. Therefore, the deposited wall is not perfectly parallel and coincident to the line formed by the thermocouples. This dimensional inaccuracy means that the reference points in the simulation are different than the actual locations of thermocouples. However, this inaccuracy is within a displacement of 2 mm. Nevertheless, this positioning error causes the peaks in the measurement to shift in time because the expected position of the torch differs from the actual position of the torch.

The simulated peak values and the ramp up to the peak values are in good agreement with the measured values. Yet, the simulated cooling behaviour differs from the measured values, clearly seen when T1.2 and S1.2 are compared in Fig. 2. The cooling is dominated by the heat loss to the environment and to the clamping. As stated previously, convection coefficient is calculated based on the measurement. Therefore, the cause of deviation is from the modelling of the clamping. Because the clamping was minimal and the plate was clamped only from two ends along the deposition axis, clamps were omitted in the simulation. However, the aim of this step was to calibrate the heat source, and the calibration was successful since the peak values for each thermocouple are in good agreement.

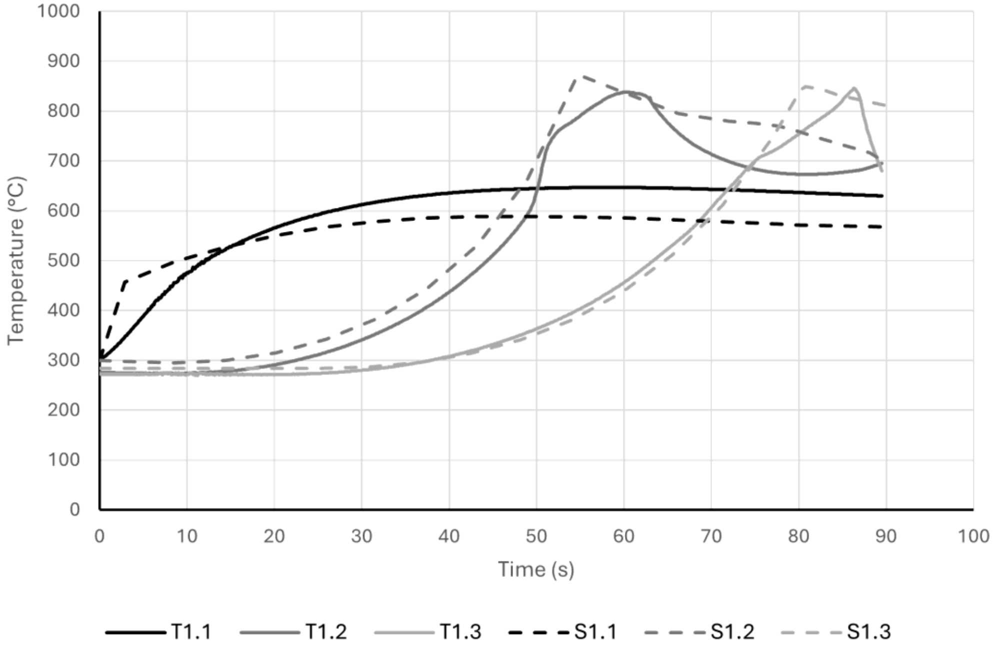

Fig. 3 Comparison of time-temperature history of the measurement (T) with simulation (S) for the calibration run

SIMULATION MODEL VALIDATION

In the simulation validation step, a new deposition process is simulated using the same heat source from the calibration step. If the calibration is done accurately, the heat source must be correct for the future processes. The danger of the calibration is to overfit the simulation to a specific case, that is the simulation is calibrated such that it gives correct results only for a given case.

In the validation experiment, the substrate is rotated by 90° along the deposition axis to print on the thin and long edge of the substrate. This orientation is used to imitate the deposited wall and match the deposition track dimensions with the substrate. The deposited wall is about 8 mm wide, and the plate is 10 mm wide. In this experiment, a new vice is used for better clamping and deposition accuracy.

The digitalization of the manufacturing process included modelling of the clamps this time because the area of contact between the clamps and the substrate is considerably larger with respect to the calibration experiment. The simulation model and the location of the thermocouples is presented in Fig. 4.

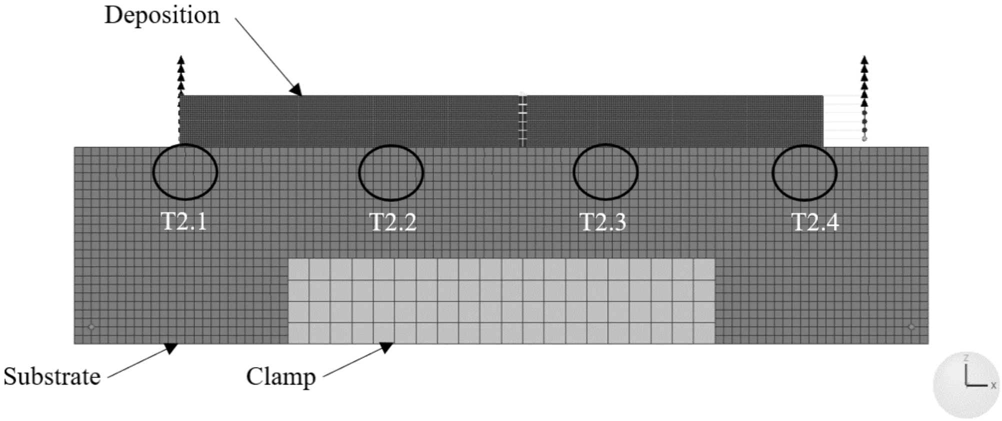

Fig. 4 Simulation model for the validation runs. Thermocouples T2.1-4 are welded to the substrate from the side surface.

The validation simulations were conducted multiple times for the mesh sensitivity analysis only. The heat source dimensions were not changed since the heat source is calibrated for the given system. The comparison of the time-temperature measurement and simulated values for the first four layers of deposition is presented in Fig. 5.

In the simulations, the cooling behaviour is not accurately predicted because of the simplified clamping model. In the experimental setup, clamping is significantly larger and more complex than the simulated blocks, as shown in Fig. 4. The clamping model used in the simulation is a representative model because the original clamping has a complex geometry with respect to substrate and deposition. To have a reasonable processing time, this simplified model of clamping is utilized in the simulation. Therefore, in the first layer, simulation predicted overcooling and as the simulation progresses, clamps saturate with heat and cannot absorb as much heat as in the beginning. Hence, from the end of the layer 3, simulations predicted undercooling. Nevertheless, the peak temperatures of the measurements and simulations are in good agreement. There is a temporal shift between the peaks of measurements and simulations. In the experiments, the torch does not turn on instantaneously but requires a time about 5 seconds to ignite. This delay causes a mismatch between the measurements and simulations.

In conclusion, the validation experiment demonstrates that the heat source calibration is done successfully as the measured and simulated temperatures are in good agreement in the validation experiment. This shows that the calibrated heat source is not overfitted to a specific deposition case and the digital model of the manufacturing system is created.

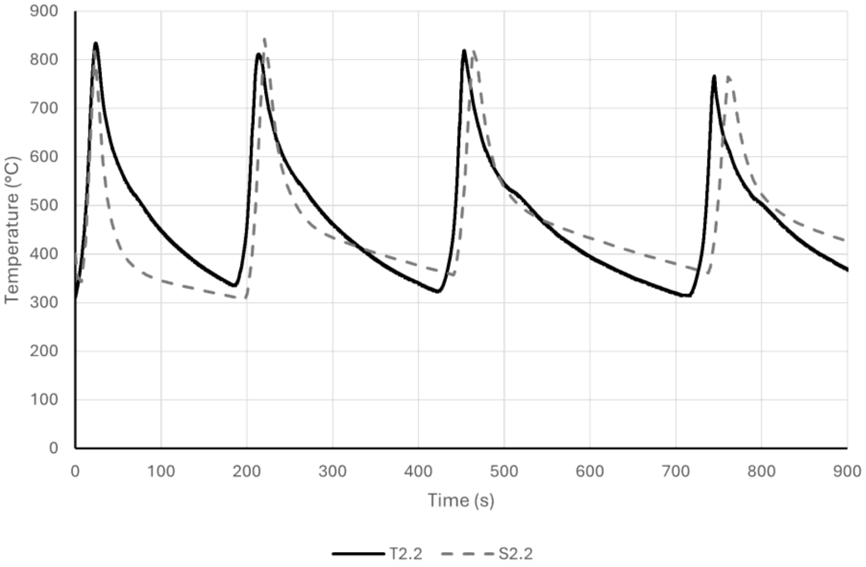

Fig. 5 Comparison of time-temperature history of the measurement (T) with simulation (S) in the validation run for the first four layers

MODELLING AND SIMULATION OF A MULTI-MATERIAL PROCESS

To combine the high thermal conductivity of copper with the structural integrity of nickel, multi-material directed energy deposition can be utilized. A structure made of functionally graded material is manufactured with the same experimental setup by combining CuCrZr powder with IN718 powder according to prescribed rates. The transition from CuCrZr to IN718 is done with an intermediate layer which is composed of 50% CuCrZr and 50% IN718 by weight.

The wall built in the experiment is composed of six layers. It begins with two layers of CuCrZr, followed by two layers of 50% Cu 50% Ni alloy, finally ends with two layers of IN718. In this way, an FGM structure is manufactured using 3DPMD. The schematic representation of the deposition process is presented in Fig. 6.

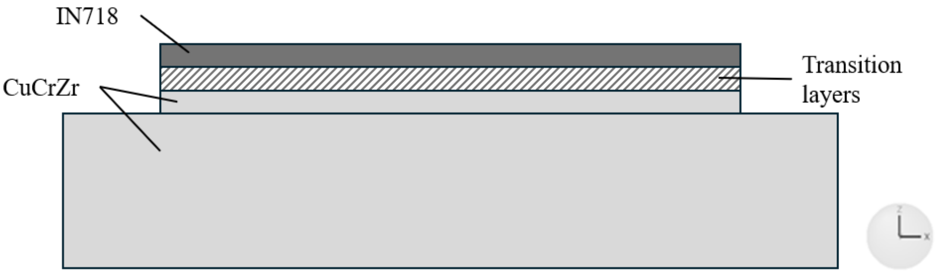

Fig. 6 Schematic representation of multi material deposition. Each material zone are composed of two layers. The transition zone composed of 50% CuCrZr and 50% IN718 by weight.

In the simulations, a material model is created for the transition layer between copper and nickel alloy by combining the two material models for the alloys in the Simufact Material Database. This new material model is obtained by combining the material properties based on rule of mixtures. Using weight contribution of each constituent, a mixture material model is obtained. This approach assumes that both materials mix perfectly in the melt pool and form a uniform phase. Since copper and nickel has fully solubility in each other, this is a valid assumption.

The simulation model for the manufacturing of the structure with FGM is presented in Fig. 7.

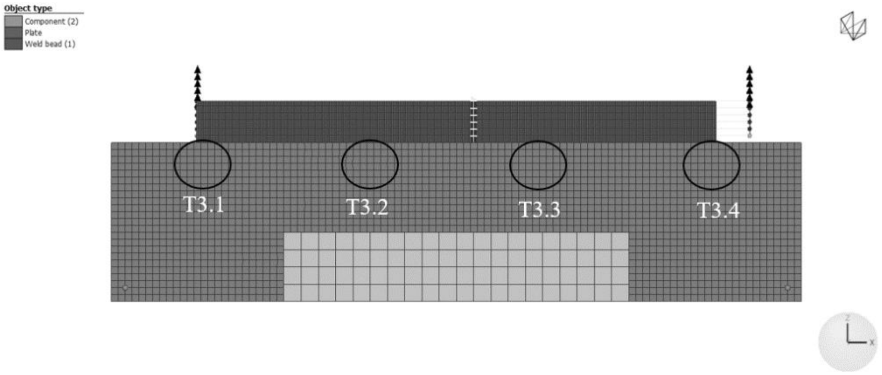

Fig. 7 Simulation model for the FGM structure. Thermocouples T3.1-4 are welded to the substrate from the side surface.

Normally, Simufact Welding interface does not allow the creation of a mixed material model or assigning more than one material to the deposition. This problem is circumvented by modifying the solver input code generated by the user interface before it is sent to the solver module. Hence, correct material models are assigned to the corresponding layers.

The time-temperature history for the second thermocouple and the simulation results from the same location are presented in Fig. 8. In the simulations, the cooling behaviour is overestimated. This effect diminishes as layers progress because in the initial layers heat loss to the clamping is overestimated. This stems from the simplified model used for the clamping solution. As the clamps heat up, the overcooling effect diminishes. Undercooling is observed at the end of the transition zone. Also, the measurement peaks for the layers five and six are 5 % and 10% smaller than the simulated values, respectively. This indicates a lack of fusion on this level, acting as thermal insulator and manifesting itself as reduced temperature increase in the measurement. However, overall, the simulation results are in good agreement with the measurements.

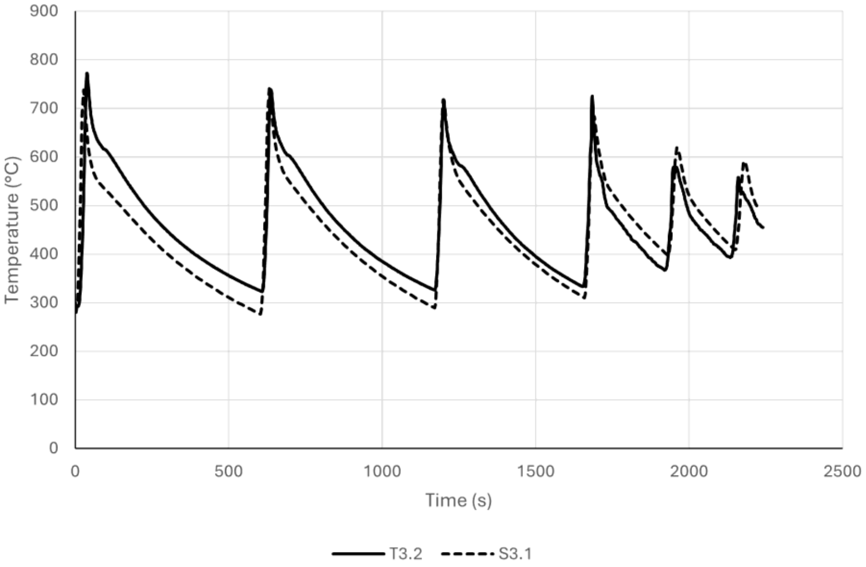

Fig. 8 Comparison of time-temperature history of the measurement (T) with simulation (S) for the multi-material deposition

CONCLUSION

This work presents a method for digitizing the multi-material 3DPMD process. Temperature evolution over time is monitored using thermocouples attached to the substrate. Time-temperature data is used to digitize the heat source, modeled as a cylinder with height equal to the layer height and diameter equal to the layer width × 1.1. Heat source power is based on experimental data, and its efficiency is calibrated to match simulation temperature peaks with measurements.

Using the demonstrated process digitalization method, once a heat source is calibrated, any DED process using the same equipment can be simulated since the digital model of the manufacturing system is obtained. This is demonstrated with the validation test and deposition of FGM.

The digital model generated in this work successfully predicts the time-temperature history of the process within a 10% error margin. The inaccuracies stem from a position error of the substrate during the experiment, and simplified modelling of the clamping solution in the simulation environment.

The capabilities of the Simufact Welding have been extended to simulate multi-material gradient deposition by manipulating the FEM code. The material properties of the gradient layers on which CuCrZr and IN718 are mixed based on the weight can be accurately modelled by combining the material properties of the constituents using the rule of mixtures.

In future work, this digital model can be further expanded by adding mechanical simulation steps to predict distortion and residual stresses. Also, the model can be used to improve process efficiency by finding a better parameter set for shorter interlayer pauses or reduced distortions.

ACKNOWLEDGEMENTS

This research was funded by the European Union‘s Horizon Europe research and innovation program, grant number 101091860 (DISCO2030).

References

[1] B. H. RABIN and I. SHIOTA: ‘Functionally Graded Materials’, *MRS Bulletin*, Vol. 20, No. 1, pp. 14-18, 1995.

[2] Z. HU, Z. MA, L. YU, Y. LIU: ‘Functionally graded materials with grain-size gradients and heterogeneous microstructures achieved by additive manufacturing’, *Scripta Materialia,* Vol. 226, 2023.

[3] S. HASANOV, S. ALKUNTE, M. RAJESHIRKE, A. GUPTA, O. HUSEYNOV, I. FIDAN, F. ALIFUI-SEGBAYA, A. RENNIE: ‘Review on Additive Manufacturing of Multi-Material Parts: Progress and Challenges’, *Journal of Manufacturing and Materials Processing*, Vol. 6, No. 1, 2022.

[4] S. YADAV, C.P. PAUL, A. K. RAI, R. SINGH, S. K. DIXIT: ‘Elucidating laser directed energy deposition based additive manufacturing of copper-stainless steel functionally graded material: Processing and material behavior’, *Journal of Manufacturing Processes*, Vol. 92, pp. 107-123, 2023.

[5] M J. SAGONG, E. S. KIM, J. M. PARK, G. M. KARTHIK, B.-J. LEE, J.-W. CHO, C. S. LEE, T. NAKANO, H. S. KIM: ‘Interface characteristics and mechanical behavior of additively manufactured multi-material of stainless steel and Inconel’, *Materials Science and Engineering: A*, Vol. 847, 2022.

[6] S. MAO, D. Z. ZHANG, Z. REN, G. FU, X. MA: ‘Effects of process parameters on interfacial characterization and mechanical properties of 316L/CuCrZr functionally graded material by selective laser melting’, *Journal of Alloys and Compounds*, Vol. 899, 2022.

[7] T. BUNTY and S. SHIVA: ‘Microstructure evolution in steel/copper graded deposition prepared using wire arc additive manufacturing’, *Materials Letters*, Vol. 380, 2022.

[8] Y. MIAO, C. LI, Y. ZHAO, Y. WU, J. LIU, Z. WANG, B. ZHANG: ‘Material properties of gradient copper-nickel alloy fabricated by wire arc additive manufacturing based on bypass-current PAW’, *Journal of Manufacturing Processes*, Vol. 83, pp. 637-649, 2022.

[9] E. R. DENLINGER, J. IRWIN, P. MICHALERIS: ‘Thermomechanical Modeling of Additive Manufacturing Large Parts’, *Journal of Manufacturing Science and Engineering*, Vol. 136, No. 6, 2014.

[10] M. CHIUMENTI, M. CERVERA, A. SALMI, C. AGELET DE SARACIBAR, N. DIALAMI, K. MATSUI: ‘Finite element modeling of multi-pass welding and shaped metal deposition processes’, *Computer Methods in Applied Mechanics and Engineering*, Vol. 199, No. 37-40, pp. 2343-2359, 2010.

[11] Q. ZHU, Z. LIU, J. YAN: ‘Machine learning for metal additive manufacturing: predicting temperature and melt pool fluid dynamics using physics-informed neural networks’, *Computational Mechanics*, Vol. 67, No. 2, pp. 619-635, 2021.

[12] M. BIEGLER, B. A. M. ELSNER, I. NEUBAUER, J. LEMKE, M. RETHMEIER: ‘Result quality evaluation of Directed Energy Deposition Additive Manufacturing simulations with progressive simplification of transient heat-source motion’, *Procedia CIRP*, Vol. 111, pp. 277-281, 2022.

[13] L. LI, X. ZHANG, W. CUI, F. LIOU, W. DENG, W. LI: ‘Temperature and residual stress distribution of FGM parts by DED process: modeling and experimental validation’, *The International Journal of Advanced Manufacturing Technology*, Vol. 109, No. 1-2, pp. 451-462, 2020.

[14] T. L. BERGMAN, A. LAVINE, F. P. INCROPERA: *Fundamentals of heat and mass transfer*, 2019.